

Optical and electrical characterizations of graphene nanoplatelet coatings on low density polyethylene

Mariano Palomba, Angela Longo, Gianfranco Carotenuto, Ubaldo Coscia, Giuseppina Ambrosone, Giulia Rusciano, Giuseppe Nenna, Gianni Barucca, and Luigi Longobardo

Citation: *Journal of Vacuum Science & Technology B, Nanotechnology and Microelectronics: Materials, Processing, Measurement, and Phenomena* **36**, 01A104 (2018);

View online: <https://doi.org/10.1116/1.4998570>

View Table of Contents: <http://avs.scitation.org/toc/jvb/36/1>

Published by the [American Vacuum Society](#)



Instruments for Advanced Science

Contact Hiden Analytical for further details:

W www.HidenAnalytical.com

E info@hiden.co.uk

CLICK TO VIEW our product catalogue



Gas Analysis

- › dynamic measurement of reaction gas streams
- › catalysis and thermal analysis
- › molecular beam studies
- › dissolved species probes
- › fermentation, environmental and ecological studies



Surface Science

- › UHV TPD
- › SIMS
- › end point detection in ion beam etch
- › elemental imaging - surface mapping



Plasma Diagnostics

- › plasma source characterization
- › etch and deposition process reaction
- › kinetic studies
- › analysis of neutral and radical species



Vacuum Analysis

- › partial pressure measurement and control of process gases
- › reactive sputter process control
- › vacuum diagnostics
- › vacuum coating process monitoring

Optical and electrical characterizations of graphene nanoplatelet coatings on low density polyethylene

Mariano Palomba, Angela Longo, and Gianfranco Carotenuto

Institute for Polymers, Composites and Biomaterials-National Research Council, Piazzale E. Fermi, 1-80055 Portici (Na), Italy

Ubaldo Coscia,^{a)} Giuseppina Ambrosone, and Giulia Rusciano

Department of Physics "Ettore Pancini," University of Naples "Federico II," via Cinthia, 80126 Napoli, Italy

Giuseppe Nenna

ENEA-Italian National Agency for New Technologies, Energy and Sustainable Economic Development, Research Centre Portici, Piazzale E. Fermi, 1-80055 Portici (Na), Italy

Gianni Barucca

Department of Materials, Engineering and Environmental Sciences and Urban Planning (SIMAU), Polytechnic University of Marche, via Brece Bianche, 60131 Ancona, Italy

Luigi Longobardo

Department of Chemical Science, University of Naples "Federico II", via Cinthia 4, 80126 Naples, Italy

(Received 1 August 2017; accepted 18 October 2017; published 6 November 2017)

Coatings of graphene nanoplatelets (GNPs) were deposited on a low density polyethylene (LDPE) substrate by a micromechanical method based on rubbing graphite platelets against the surface of the polymer. Transmission electron microscopy measurements reveal that the coatings were composed of nanoplatelets containing 13–30 graphene layers. Thermal gravimetric analysis shows that the investigated GNP coatings on LDPE (GNP/LDPE) samples are thermally stable up to 250 °C. Optical spectra of these samples, compared to those of pristine LDPE in the ultraviolet-visible-near-infrared range, indicate an increase in both reflectance and absorptance. On the other hand, the coating is able to markedly improve the surface conductivity of the polymeric substrate, indeed in the case of electrical contacts in the coplanar configuration (1 cm long and spaced 1 mm), the resistance of LDPE is $10^{15} \Omega$, while that of GNP/LDPE is 670Ω . Electrical measurements under white light illumination point out a decrease in the conductance and a linear behavior of the photoconductance as a function of the optical power density. GNP/LDPE materials can be used for their optical, electrical, thermal, and flexibility properties in large area plastic electronics and optoelectronics. *Published by the AVS.* <https://doi.org/10.1116/1.4998570>

I. INTRODUCTION

Nowadays, flexible electronics offers numerous advantages such as large area production, low cost, and environmental perspectives, and it does not require high temperature processes. Plastics (both linear polymers and resins) are technologically important materials in this field because they have many useful characteristics, such as low specific weight, high strength/weight ratio, and easy processing.^{1–3} However, many of these synthetic materials have inherently low thermal and electrical conductivities which limit their applications. Although conductive polymers (polyaniline, poly(3,4-ethylenedioxythiophene), etc.) can be synthesized, their low mechanical/chemical performance makes difficult the industrial exploitation.⁴ Currently, the filling of nonconductive polymers with inert and conductive/semiconductive additives, such as sp^2 carbon-based materials^{5,6} (graphite, carbon nanotube, graphene, etc.), is an effective and inexpensive method to produce conductive composites.^{7,8} In fact, these materials provide electrical conduction through the π bonding system extending between adjacent carbon atoms in their chemical structure, whereas thermal

conduction derives also from the overlapping of sigma-bonds belonging to the same molecular bonding system.⁹ However, to obtain a conductive composite, it is necessary to reach the percolation threshold that allows continuous pathways of inter-connected conductive particles through the dispersing polymeric phase.¹⁰

A completely different approach to the fabrication of conductive polymeric materials has been proposed by Huang *et al.*¹¹ that used graphene multilayers as coatings on the surface of plastic substrates. They deposited an ink of graphene nanoflakes on polyethylene terephthalate and, after drying and compression rolling treatments, obtained a conductive graphene laminate.

A simple and effective micromechanical approach, without any postdeposition treatments, has been recently proposed by Coscia *et al.*¹² They have deposited graphene nanoplatelet (GNP) coating on the surface of a soft polymeric substrate such as low density polyethylene (LDPE) by rubbing some graphite platelet paste between two sheets of this polymer. This procedure produces a combination of opposite tangential mechanical stresses, such as shear and friction forces, that can easily detach weakly bonded GNP from graphite platelets. This micromechanical process could be easily scaled up by adapting

^{a)}Electronic mail: coscia@fisica.unina.it

technologies already existing in industry. Electrically conductive GNP coatings can be very useful to make tracks for printed circuit boards in plastic electronics and optically transparent electrodes for optoelectronics, replacing indium tin oxide and other much more expensive traditional materials.¹³

In this paper, the morphological, thermal, structural, optical, and electrical properties of the graphene nanoplatelets deposited on the LDPE substrate (GNP/LDPE) using the above micromechanical techniques are presented and compared with those of the pristine LDPE.

II. EXPERIMENT

The pristine LDPE used for the experiments was a commercial film provided by Sabich (99.77% by weight, $M_n = 280\,000\text{ g mol}^{-1}$, melt flow index = 7 g/10 min, and thickness $\sim 42\text{ }\mu\text{m}$). Specimens of large area ($20 \times 30\text{ cm}$) were prepared by coating LDPE films using the following micromechanical method. First, dry graphite platelets were accurately mixed with pure ethanol (Aldrich, 99.9%) using a sonication bath, and then, this liquid colloidal dispersion was concentrated by solvent evaporation (under sonication) at room temperature to achieve a soft paste. A little amount of this paste was placed on the LDPE surface (firmly fixed to a flat glass) and was accurately spread using a similar LDPE film as counterface, by applying a pressure ranging from 3 to 9 kPa. Soft nonpolar polymers (such as polyethylene, silicon rubbers, amorphous ethylene-propylene copolymers, etc.) can provide enough friction to cause the exfoliation of the graphite platelets. The thickness of the deposited coating can be controlled by varying the amount of paste spread on the surface area. More details were reported in Coscia *et al.*¹² Samples sized $1 \times 1\text{ cm}$ were obtained from a large specimen ($20 \times 30\text{ cm}$) for the different characterizations.

Scanning electron microscopy (SEM) images of the samples were obtained using a FEI Quanta 200 FEG microscope. Transmission electron microscopy (TEM) images were obtained using a Philips CM200 microscope operating at 200 kV and equipped with a LaB₆ filament. For TEM observations, samples were prepared in cross-section by using a Leica EM UC6/FC6 cryo-ultramicrotome.

The thermal gravimetric analysis (TGA) was performed on LDPE, GNP/LDPE, and GNP residues derived from the deposition, by using a TA Instruments Q500, operating in nitrogen flow with a constant rate of $10\text{ }^\circ\text{C/min}$.

Raman spectra were acquired by using a WiTec, alpha 300 apparatus, consisting of a confocal microscope endowed with an excitation source at 532 nm, supplied by a Nd:YAG laser. Spectra were recorded over the range of $300\text{ to }3000\text{ cm}^{-1}$ with a spectral resolution of 3.6 cm^{-1} . Raman measurements were carried out on LDPE, GNP/LDPE, and residues of GNP coating extracted by dissolving the LDPE substrate with boiling xylene.

Transmittance and reflectance spectra were obtained for LDPE and GNP/LDPE samples in the $200\text{--}2500\text{ nm}$ range with an acquisition rate of 1 nm/s , using a Perkin-Elmer Lambda 900 spectrophotometer, equipped with an integrating sphere (diameter of 15 cm) covered by Spectralon.

The electrical measurements of the substrate LDPE and GNP/LDPE samples were performed at room temperature, in a coplanar configuration by silver paint contacts (1 cm long and spaced 1 mm) deposited on their surfaces. The bias voltage was applied by means of a Tektronics PS 280 DC power supply or a Keithley 247 high voltage supply, and the current was measured by using a Keithley 6485 picoammeter equipped with a general purpose interface bus interface and custom-made LABVIEW application. Current versus time acquisitions of GNP/LDPE were recorded switching on and off the white light illumination of a 450 W Xenon lamp (ILC Technology), varying the applied voltage between -120 and 120 mV and the optical power density in the $20.9\text{--}286.2\text{ mW/cm}^2$ range. The optical power density of light irradiation was measured using a Laser precision Rk-5720 power radiometer.

III. RESULTS AND DISCUSSION

The modification of the surface morphology, due to the micromechanical deposition process, is illustrated in the sequence of SEM-micrographs given in Fig. 1. Figure 1(a) shows that the LDPE surface is flat, with very long scratches and few little blisters as defects, probably generated during the film fabrication process (blow molding). In the course of the coating treatment, the surface is progressively covered, as displayed in Fig. 1(b), where the defects are filled but still visible. At the end of the process, the LDPE surface is completely covered [Fig. 1(c)].

In order to investigate the inner structure of the coating deposited on the LDPE, TEM analysis was performed on cross-sectioned samples. In the TEM image in Fig. 2(a), the LDPE substrate and the overlying coating, about 20 nm thick, are clearly visible. In Fig. 2(b), the details of the arrowed region in Fig. 2(a) are presented: the coating is composed of graphene nanoplatelets which are quite parallel to the substrate and are formed by the overlap of 13–14 graphene layers, separated by a distance of $d = (0.35 \pm 0.02)\text{ nm}$.

A detailed analysis of different regions of the large area sample showed that the coating thickness ranged from 5 to 90 nm and that nanoplatelets were typically thicker near the LDPE substrate (13–30 graphene layers) and thinner at the top of the coating.

Thermogravimetric analysis was carried out to characterize the thermal properties of the GNP/LDPE sample. For comparison, TGA tests were also performed on pristine LDPE and residues of GNP derived from the coating deposition. The samples were heated in a TGA instrument up to $800\text{ }^\circ\text{C}$ with a heating rate of $10\text{ }^\circ\text{C min}^{-1}$ under nitrogen. As shown in Fig. 3, the GNP/LDPE sample was thermally stable up to a temperature of $\sim 250\text{ }^\circ\text{C}$, and then, it decreased in weight by 8% at $400\text{ }^\circ\text{C}$. In the $400\text{--}500\text{ }^\circ\text{C}$ range, although the weight of GNP decreased slightly, the thermal behavior of the GNP/LDPE sample was the same as that of the pristine LDPE and the weight decreased from $\sim 92\%$ to $\sim 1\%$ because of the complete decomposition of the substrate. The percentage by weight of GNP in the GNP/LDPE system was estimated to be 0.41% by the difference between the GNP/

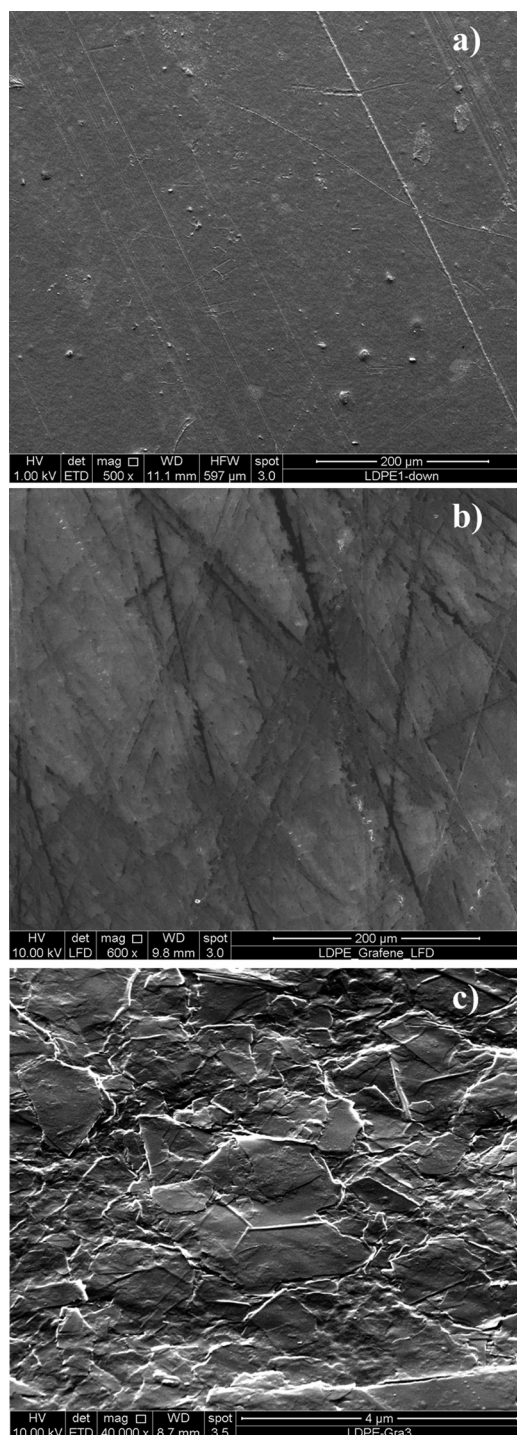


FIG. 1. SEM-micrographs of (a) LDPE substrate; (b) partially coated LDPE substrate; (c) fully coated LDPE substrate.

LDPE and pure LDPE residual weights. Clearly, the amount of deposited coating is extremely low as compared to that of LDPE substrate, and this is the reason for the thermal behavior of the polymer is dominant and the TGA curves of LDPE and GNP/LDPE almost overlap in the full temperature range.

It is worth noting that the weight of the GNP residues continued to decrease slowly even in the 500–800 °C range, reaching 91%, demonstrating the good thermal properties of

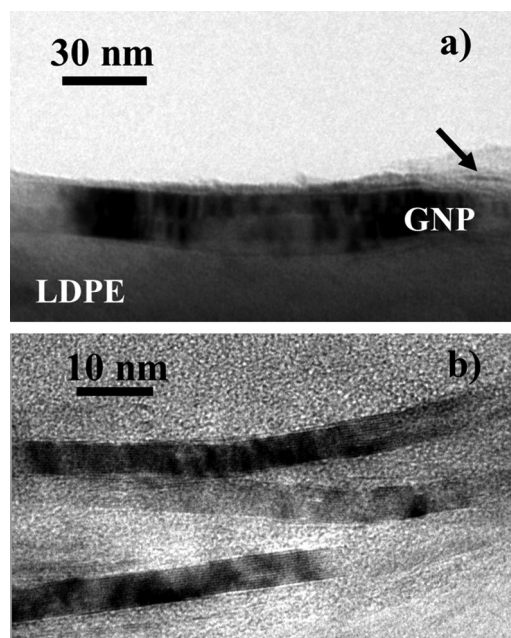


FIG. 2. TEM images of the cross-sectioned graphene nanoplatelets on the LDPE substrate: general view (a); details of the arrowed region (b).

the deposited GNP. Therefore, the GNP thermal stability is comparable with that of other types of graphene coatings, produced by different techniques.⁵

The structural properties of LDPE, GNP/LDPE, and GNP samples were investigated by Raman spectroscopy. Figure 4(a) shows the spectrum displaying the typical bands of LDPE (Refs. 8 and 14) centered at 1299 and 1454 cm^{-1} assigned to *all-trans* $-(\text{CH}_2)-$ groups and to the anisotropic parts of the polymer, respectively. Further, two more bands at 2842 and 2879 cm^{-1} can be attributed to C-H (methyl) stretching vibrations. The positions of the band assignments are marked by dashed lines as guides to the eye. In Fig. 4(b), it can be seen that the GNP/LDPE Raman spectrum is affected by a higher level of noise. In addition to the above described LDPE bands, three more bands can be observed at around 1358, 1580, and 2680 cm^{-1} , due to D, G, and 2D bands of the GNP coating, respectively.^{15–17} The D-band can be attributed to the amount of disorder/defects in the structure, while the G band originates from in-plane bond stretching of

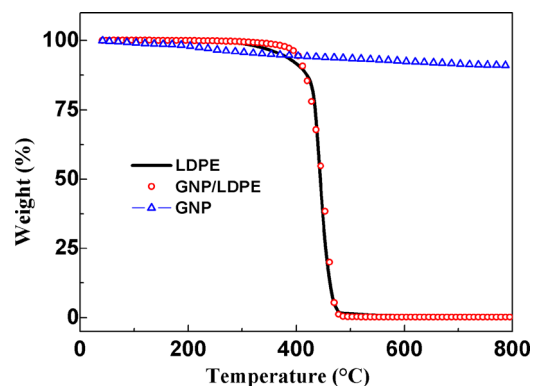


FIG. 3. (Color online) TGA curves of the pristine LDPE, GNP/LDPE samples, and residues of GNP coating.

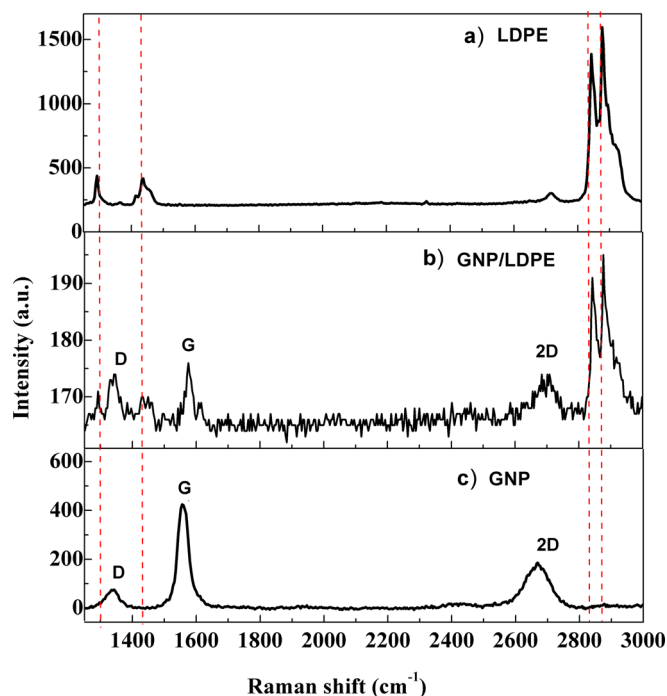


FIG. 4. (Color online) Raman spectra of the LDPE substrate (a); GNP/LDPE sample (b); and GNP coating (c). The dashed lines indicate the positions of the typical bands of LDPE.

sp²-C atoms that can be assigned to doubly degenerate phonon mode E_{2g} symmetry. Finally, the 2D band is the overtone of the D band, and it reflects the number of graphene layers.^{18,19}

In order to get more information on the structure of GNP coating, the LDPE substrate was removed from the sample by dissolving it with boiling xylene. The Raman spectrum of the achieved GNP coating residues is shown in Fig. 4(c). The D, G, and 2D bands appear clearly defined, and their intensities can be better evaluated. Indeed, the ratio of the D peak intensity to that of the G peak is about 0.17, revealing a low degree of disorder in the deposited coating, while the ratio of the 2D peak intensity to that of the G peak is about 0.44, indicating a structure based on graphene multilayers,¹⁹ according to TEM analysis.

Figure 5 shows the diffuse reflectance, R_d , spectra of LDPE and GNP/LDPE samples, in the UV-Vis-near-infrared (NIR) spectral range (200–2500 nm). The two spectra are very different in the UV region; indeed, R_d decreases for the LDPE substrate, while, in the case of the GNP/LDPE sample, it shows an intense and narrow peak, centered at ~250 nm, due to the surface plasmon resonance of graphene nanoplatelets.^{20,21} In the 500–2000 nm range, R_d is constant for both samples at around 5% and 15%, respectively, and then, it slightly decreases in the 2000–2500 nm range.

The total reflectance, R_T , spectra of the above samples, in the UV-Vis-NIR range, are shown in Fig. 6. R_T of the LDPE substrate decreases in the UV region and exhibits a constant value of about 7% in the Vis-NIR range, while R_T of the GNP/LDPE sample increases in the Vis-NIR region and shows a peak centered at ~250 nm in the UV region, as in the case of R_d spectra. From the different behavior of R_T and R_d of the GNP/LDPE sample in the Vis-NIR region, it can

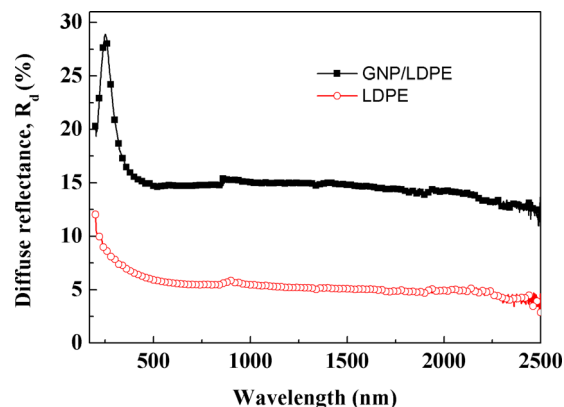


FIG. 5. (Color online) Diffuse reflectance, R_d , spectra of GNP/LDPE and LDPE samples.

be argued that the specular reflectance increases with the wavelength.

In fact, in Fig. 7, it can be seen that the specular reflectance, obtained by subtracting the diffuse to the total reflectance, linearly increases from 6.4% to 14% for GNP/LDPE, while it is almost constant at ~2.5% for the pristine LDPE.

The transmittance spectra, T , are shown in Fig. 8. In the UV range, the transmittance of LDPE strongly increases from 13% to 80%, while in the GNP/LDPE spectrum, the typical peak related to the surface plasmon resonance of GNP can be identified at about 250 nm. Furthermore, in the NIR range (2300–2350 nm), the absorption bands, due to the second overtone of the CH₂ bending mode of the LDPE, appear evident in both spectra.²² In the Vis-NIR range (500–2000 nm), the transmittance of LDPE and GNP/LDPE samples is approximately constant at ~87% and ~25%, respectively. Therefore, in this range, the absorbance, A , defined as $A = 100 - R_T - T$, varies in 4%–8% and 45%–58% ranges for LDPE and GNP/LDPE, respectively. This analysis indicates that a thin GNP coating is able to significantly modify the optical properties of the LDPE substrate by increasing both total reflectance and absorbance.

The electrical measurements of pristine LDPE and GNP/LDPE samples were performed in the coplanar configuration. The resistance of the LDPE substrate in dark conditions

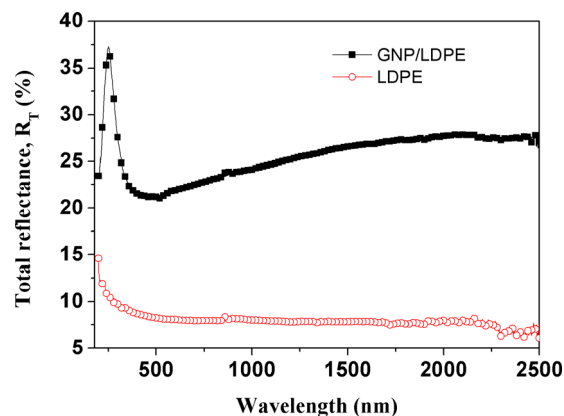


FIG. 6. (Color online) Total reflectance, R_T , spectra of GNP/LDPE and LDPE samples.

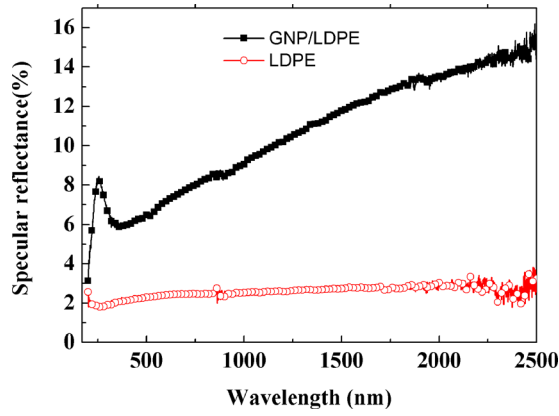


FIG. 7. (Color online) Specular reflectance spectra of GNP/LDPE and LDPE samples.

was evaluated to be $\sim 10^{15} \Omega$ [see the I-V characteristic in Fig. 9(a)], while, after depositing the graphene nanoplatelet coating, a strong improvement in the surface conductivity properties was found because the resistance of GNP/LDPE was 670Ω [see the I-V characteristic in Fig. 9(b)].

In order to determine the electrical response to the white light, the GNP/LDPE sample was illuminated by varying the optical power density, F , of a xenon lamp in the 20.9 – 286.2 mW/cm^2 range. The sample was subjected to dark-light cycles at fixed F values with a light exposure time of 300 s . The photoconductivity properties are described, in the following, by means of the photoconductance G_{ph} , determined as

$$G_{ph} = G_{light} - G_{dark},$$

where G_{dark} and G_{light} are the conductances in dark conditions (before turning on the light) and under illumination, respectively.

From data analysis, it was found that G_{ph} was independent of the applied voltage in the investigated range (from -120 to 120 mV). The time-dependent photoconductance at different optical power densities, F , is displayed in Fig. 10. Clearly, the sample under white light shows a negative photoconductivity.^{23,24} Also, Shi *et al.*²⁵ and Biswas *et al.*²⁶

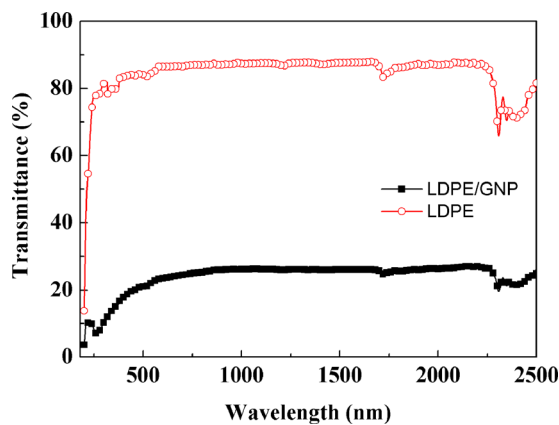


FIG. 8. (Color online) Transmittance spectra of GNP/LDPE and LDPE samples.

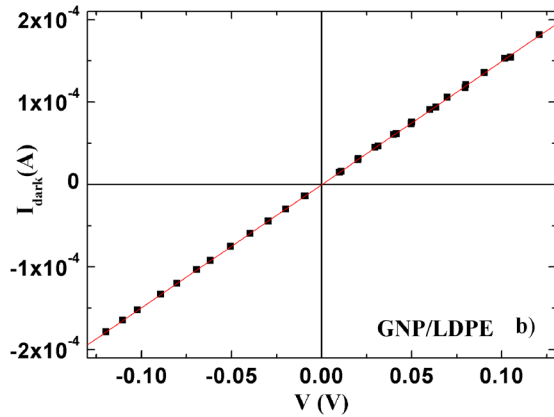
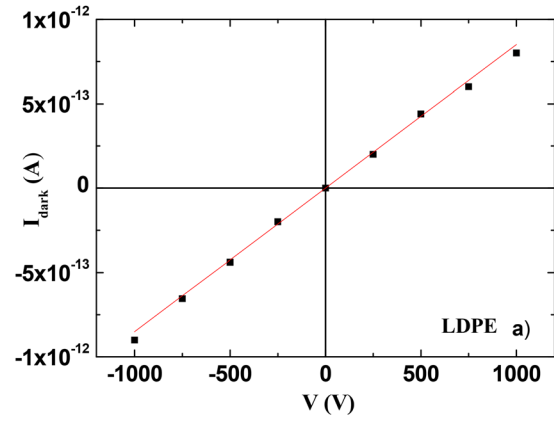


FIG. 9. (Color online) I-V characteristics of LDPE substrate (a); and GNP/LDPE sample (b).

found negative photoconductivity in graphene layers under white light and radiation of different wavelengths, respectively. These authors attributed the decrease in conductivity under illumination to the photodesorption of hydroxyl groups and/or molecular O_2 .

To gain a better insight into this process, the photoconductance recorded after 300 s of illumination, G_{phf} , of all the measurements is plotted versus the optical power density in Fig. 11. The trend of G_{phf} as a function of F is well fitted by the linear function

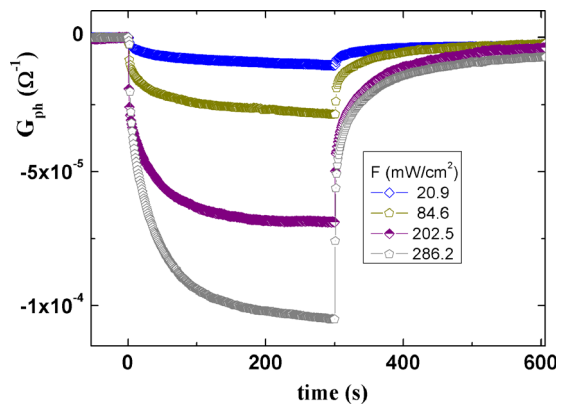


FIG. 10. (Color online) Time dependent photoconductance, G_{ph} , at different optical power densities, F .

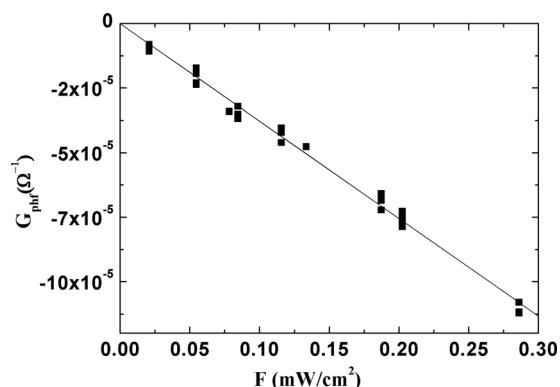


FIG. 11. Photoconductance after 300 s of illumination, G_{phf} , as a function of optical power density F .

$$G_{phf} = kF,$$

where $k = -3.623 \times 10^{-4} \pm 3.4 \times 10^{-6} \text{ cm}^2 \Omega^{-1} \text{ W}^{-1}$ is obtained with a correlation coefficient $r = 0.991$

IV. SUMMARY AND CONCLUSIONS

Coatings of overlapping nanoplatelets composed of 13–30 graphene layers were deposited on the LDPE substrate by a micromechanical technique. This method is based on the application of shear and friction forces to a graphite platelets/ethanol paste on the surface of the polymeric substrate. The TGA shows that the GNP/LDPE structure is thermally stable up to 250 °C. It has been demonstrated that a coating of graphene nanoplatelets is able to significantly modify the optical and electrical properties of the polymeric surface. Indeed, in the case of the investigated GNP/LDPE sample, the coating increases both the diffuse and total reflectance, giving rise to a linear increase in the specular reflectance from 6.4% to 14% in the Vis-NIR region, while that of the pristine LDPE remains almost constant at around 2.5%. In the same spectral range, the coating markedly decreases the transmittance from 87% to 25%, leading to an increase in the absorptance from 4%–8% to 45%–58%. On the other hand, the graphene nanoplatelets strongly improve the surface conductivity properties. In fact, the resistance of the LDPE substrate as compared to that of the GNP/LDPE sample decreases by more than 12 orders of magnitude. Electrical measurements of the GNP/LDPE sample, performed under white light cycles, put in evidence a decrease in the conductance and a linear behavior of photoconductance as a function of optical power density. GNP/LDPE for

its properties could be advantageously used as a semitransparent/conductive material for large area plastic electronics and optoelectronics.

ACKNOWLEDGMENT

The authors gratefully acknowledge Maria Cristina del Barone of the LAMEST laboratory IPCB-CNR for the SEM and TEM measurements.

- ¹M. Kaltenbrunner *et al.*, *Nature* **499**, 458 (2013).
- ²Y. L. Loo, R. L. Willett, K. W. Baldwin, and J. A. Rogers, *Appl. Phys. Lett.* **81**, 562 (2002).
- ³B. Singh and N. S. Sariciftci, *Annu. Rev. Mater. Res.* **36**, 199 (2006).
- ⁴R. Balint, N. J. Cassidy, and S. H. Cartmell, *Acta Biomater.* **10**, 2341 (2014).
- ⁵J. Wang *et al.*, *J. Nanopart. Res.* **13**, 869 (2011).
- ⁶N. Garcia, P. Esquinazi, J. Barzola-Ququia, and S. Dusari, *New J. Phys.* **14**, 053015 (2012).
- ⁷G. D. Liang and S. C. Tjong, *Mater. Chem. Phys.* **100**, 132 (2006).
- ⁸A. A. Vasileiou, M. Kontopoulou, and A. Docoslis, *ACS Appl. Mater. Interfaces* **6**, 1916 (2014).
- ⁹H. Lei *et al.*, *RSC Adv.* **6**, 101492 (2016).
- ¹⁰C. W. Nan, *Prog. Mater. Sci.* **37**, 1 (1993).
- ¹¹X. Huang, T. Leng, X. Zhang, J. C. Chen, K. H. Chang, A. K. Geim, K. S. Novoselov, and Z. Hu, *Appl. Phys. Lett.* **106**, 203105 (2015).
- ¹²U. Coscia, M. Palomba, G. Ambrosone, G. Barucca, M. Cabibbo, P. Mengucci, R. de Asmundis, and G. Carotenuto, *Nanotechnology* **28**, 194001 (2017).
- ¹³R. K. De Castro, J. R. Araujo, R. Valaski, L. O. O. Costa, B. S. Archanjo, B. Fragneaud, M. Cremona, and C. A. Achete, *Chem. Eng. J.* **273**, 509 (2015).
- ¹⁴H. Sato, M. Shimoyana, T. Kamiya, T. Amari, S. Šašić, T. Ninomiya, H. W. Siesler, and Y. Ozaki, *J. Appl. Polym. Sci.* **86**, 443 (2002).
- ¹⁵A. C. Ferrari and D. M. Basko, *Nat. Nanotechnol.* **8**, 235 (2013).
- ¹⁶A. C. Ferrari *et al.*, *Phys. Rev. Lett.* **97**, 187401 (2006).
- ¹⁷A. C. Ferrari, *Solid State Commun.* **143**, 47 (2007).
- ¹⁸E. H. Martinez Ferreira, M. V. O. Moutinho, F. Stavale, M. M. Lucchese, R. B. Capaz, C. A. Achete, and A. Jorio, *Phys. Rev. B* **82**, 125429 (2010).
- ¹⁹A. Das, B. Chakraborty, and A. K. Sood, *Bull. Mater. Sci.* **31**, 579 (2008).
- ²⁰E. A. Taft and H. R. Philipp, *Phys. Rev.* **138**, A197 (1965).
- ²¹G. I. Dovbeshko, V. R. Romanyuk, D. V. Pidgirnyi, V. V. Cherepanov, E. O. Andreev, V. M. Levin, P. P. Kuzhir, T. Kaplas, and Y. P. Svirko, *Nanoscale Res. Lett.* **10**, 234 (2015).
- ²²W. Kossack, P. Papadopoulos, M. Parkinson, F. Prades, and F. Kremer, *Polymer* **52**, 6061 (2011).
- ²³M. Palomba, M. Salvatore, G. Carotenuto, U. Coscia, G. Ambrosone, and S. De Nicola, *IEEE 15th International Conference on Nanotechnology (IEEE-NANO)* (2015), p. 485.
- ²⁴U. Coscia, M. Palomba, G. Ambrosone, G. Barucca, and G. Carotenuto, *18th Italian National Conference on Photonic Technologies* (2016).
- ²⁵Y. Shi, W. Fang, K. Zhang, W. Zhang, and L. J. Li, *Small* **5**, 2005 (2009).
- ²⁶C. Biswas, F. Gunes, D. D. Loc, S. C. Lim, M. S. Jeong, D. Pribat, and Y. H. Lee, *Nano Lett.* **11**, 4682 (2011).